High Frequency of Cryptic Deleterious Mutations in *Caenorhabditis elegans*

Esther K. Davies, Andrew D. Peters, Peter D. Keightley*

Deleterious mutations with very small phenotypic effects could be important for several evolutionary phenomena, but the extent of their contribution has been unknown. Fitness effects of induced mutations in lines of *Caenorhabditis elegans* were measured using a system for which the number of deleterious point mutations in the DNA can be estimated. In fitness assays, only about 4 percent of the deleterious mutations fixed in each line were detectable. The remaining 96 percent, though cryptic, are significant for mutation load and, potentially, for the evolution of sex.

The prevalence of sexual reproduction may be explicable by the ability of sexual populations to sustain higher rates of deleterious mutation than asexuals (*1*). However, it has been argued that the accumulation of deleterious mutations could lead to fitness loss and ultimately to population extinction, even in sexual species, if effective population size is small (*2*). Mutation accumulation experiments in *Drosophila* suggest that mutations with harmful effects of the magnitude required for this fitness loss (~1%) occur frequently (*3*), but joint estimates of the spontaneous genomic deleterious mutation rate, U, and the mean deleterious mutation effect, s, from these experiments have been questioned (*4, 5*). An alternative molecular constraint approach to estimate U compares rates of nucleotide substitution in functional and neutral regions of the genome (*6*), but does not give direct information on the magnitude of mutation effects. Here, we combine the molecular constraint and mutation accumulation approaches to infer the distribution of fitness effects of point mutations in the nematode *C. elegans*.

We exposed the N2 (wild type) strain of *C. elegans* to 50 mM ethylmethane sulfonate (EMS) for 4 hours, a dosage for which the number of mutations induced at the DNA level has been calibrated (*7*). About 92% of the mutations produced by this treatment are G/C → A/T transitions; the remainder are other kinds of point mutations, plus a low frequency of small deletions (*7*). Data from experiments to measure forward mutation rates (*8*) and suppressor-induced reversion mutation rates (*9–11*) under EMS mutagenesis provide a mean estimate for the rate of transitions of 6.2×10^{-6} [95% confidence interval (CI) of (Table 1) 4.0×10^{-6} to 8.4×10^{-6}] per G/C base pair. The haploid genome of *C. elegans* is 9.7×10^7 base pairs, comprising 36% G/C (*12*), so the mutagenesis generated an expected number of 220 transition mutations per haploid. The fraction of the genome in exons is 27% (*12*), and we infer from tables of codon usage in >15,000 *C. elegans* genes (*13*) that 30.6% of nucleotides in exons are G/C and generate an amino acid change if mutated to A/T. Therefore, we estimate that the EMS treatment generated an average of $(6.2 \times 10^{-6}) \times (9.7 \times 10^7) \times 0.27 \times 0.306 = 50$ (95% CI of 32 to 68) transition mutations per haploid that changed an amino acid in a protein-coding gene. Protein-coding sequences are under strong selective constraint in *C. elegans*: Data on synonymous and nonsynonymous substitution rates in *C. elegans* and its relative *C. briggsae* (*14*) suggest that ~90% of amino acid mutations are removed by natural selection. Thus, we estimate that the minimum number of mutations induced per haploid genome that are deleterious in natural conditions is ~45, but the number could be substantially higher because some noncoding DNA is selectively constrained (*15*). A comparison of the relative levels of selection against amino acid changes [using a log-odds (Dayhoff) matrix (*16*)] arising from G/C → A/T transitions to other types of point mutations (A/T → G/C transitions and transversions) suggests that the severity of individual amino acid changes generated by EMS is similar to that of spontaneous mutations (*17*).

After the mutagenesis, we bred 60 independent EMS lines toward homozygosity by selfing. In the absence of selection, the number of mutations fixed is expected to be the number of mutations induced per haploid genome. During the inbreeding, conditions were made as favorable as possible to avoid selection. However, some backup cultures were used, and four lines were lost, implying the action of natural selection (Fig. 1) and the selective loss of some mutations (such as recessive lethals). To estimate the magnitude of this loss, we performed computer simulations of lines undergoing multiple generations of selfing, analogous to our experimental design (*18*). The mean proportion of plates producing at least one progeny (surviving cultures) among the EMS-treated lines in our experiment was 0.74, with a 95% CI of 0.68 to 0.80 (Fig. 1). Under the parameter values simulated, only mutation effects of less than 10^{-3} are predicted to lead to viabilities within this range (Fig. 1). In our simulations, if lines had 45 heterozygous mutations at the start of inbreeding, such mutation effects led to the loss of 6% of mutations or fewer, on average, to selection (Fig. 1). This suggests that at most three mutations, two of which were minor-effect mutations, were selectively lost (on average) per line. Simulations assuming that fitness declines faster than exponentially with increasing numbers of mutations (synergistic epistasis) led to similar or lower estimates of the number of mutations selectively lost (*17*).

We measured lifetime reproductive output of individual worms from the 56 surviving EMS lines and 40 control lines. This fitness measure includes the viability of the parents,

Table 1. Rates of G/C → A/T transition mutations induced by EMS. The frequency of mutations is adjusted to a dosage of 50 mM EMS for 4 hours [as used here and in (*9*)] by assuming the EMS dose-response curve of (*21*) [(*10, 11*); 25 mM EMS, 4 hours], or assuming mutation rate is linear with time [(*8*); 50 mM EMS, 3.5 hours].

Reference	Sensitive sites	Total sites screened	No. of mutations	Adjusted mutation rate per G/C ($\times 10^{-6}$)
(*8*)*	160	960,000	7	8.3
(*9*)†‡	2	1,248,000	4	3.2
(*10*)†§	6	2,400,000	9	5.2
(*11*)†§	6	1,572,000	9	8.0
Mean				6.2
				(95% CI 4.0 to 8.4)

*Screened for *unc-54* null mutants, the majority of which are nonsense alleles (*30*). The number of *unc-54* sites at which an EMS-induced transition can produce a nonsense allele is 160 (*7*). †Screened for amber suppressors caused by single base-pair changes at $tRNA^{Trp}$ genes. ‡Screened for *unc-13* extragenic suppressors, all of which mapped to two sites. §Screened for *tra-3* extragenic suppressors, and identified mutations at four and five $tRNA^{Trp}$ genes, respectively, a total of six sites.

Institute of Cell, Animal and Population Biology, University of Edinburgh, West Mains Road, Edinburgh EH9 3JT, UK.

*To whom correspondence should be addressed. E-mail: p.keightley@ed.ac.uk

their fertility, and the viability of offspring until the L3 to young adult stage. The EMS treatment reduced mean productivity by 34% (±4%), and it produced a large increase in the between-line variance (V_G) and obvious changes in the distribution of line means that are consistent across the three replicates carried out (Fig. 2). Qualitatively similar results are obtained if age-specific reproductive output is converted to an intrinsic growth rate fitness measure (*17*). As a positive control for mutagenesis, we also measured the mutation rate at the *unc-22* locus (*19*). Our estimated rate is 7.6 (±1.0) × 10^{-4} per haploid, a ~1250-fold increase over the spontaneous background rate of 6 × 10^{-7} (*20*).

Estimates of U_I, the EMS-induced mutation rate per haploid genome, and s, the homozygous effect on productivity, can be obtained from phenotypic data under a model of equal mutation effects, for which the overall change in mean fitness is $\Delta M = U_I s$ and the increase in between-line variance from mutation is $V_G = U_I s^2$ (*3*). From our productivity data, these estimates are $\hat{U}_I = \Delta M^2/V_G = 1.4$ (±0.36) and $\hat{s} = V_G/\Delta M = 24\%$ (±3.9%). The number of mutations detected is therefore only slightly higher than the number of recessive lethal mutations induced by 50 mM EMS, estimated at ~1 per haploid genome (*21, 22*). This contrasts sharply with our inference that each line contains an average of >45 deleterious point mutations. Clearly, the assumption made in these calculations that mutations have equal effects is violated.

To find distributions of mutation effects giving an improved fit to the data, we used maximum likelihood (ML) (*23*). Surprisingly, the best-fitting γ distribution is the equal-effects model (β → ∞); a γ distribution in which there are many mutations with small effects and a diminishing tail of larger effects gives a poorer fit than equal effects if the mutation rate is a variable in the model (Table 2). This result implies that the underlying distribution of mutation effects may be multimodal, because the γ distribution does not simultaneously allow a high frequency of slightly deleterious mutations and a "spike" of strongly deleterious mutations. The best-fitting model we obtained under ML, assuming our a priori estimate of $U_I = 45$, is two classes of deleterious mutation effects, the

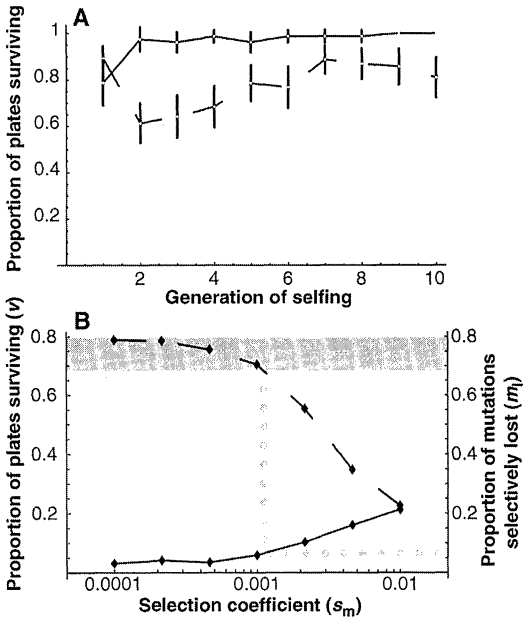

Fig. 1. The N2 strain of *C. elegans* was obtained from the *Caenorhabditis* Genetics Center. Cultures were maintained using standard techniques (*31*) at 20°C on 3.5-cm agar plates, seeded with a suspension of *E. coli* strain OP50, and allowed to grow overnight. A large, synchronous population of young adults was divided into two subpopulations. One population was mutagenized with 50 mM EMS in M9 buffer for 4 hours at 20°C according to the protocol of (*7*). The control population was treated in an identical manner, but worms were instead maintained in M9 buffer. Worms were allowed to recover on plates for 24 hours; any eggs present during the mutagenesis would therefore have been expelled and hatched. The worms were then removed by washing with M9 buffer and treated with alkaline hypochlorite to harvest eggs, which were then transferred to fresh plates. Two days later, small numbers of worms were distributed onto individual plates to start 60 mutant and 40 control lines. Mutant and control lines were then selfed for 10 generations to fix mutations. Lines were propagated in parallel by the transfer of one hermaphrodite, chosen from a random position on each plate. Backup plates (two per EMS line, one per control) were used in cases where the parent failed to produce progeny. If no replicate produced offspring, a worm was substituted from the plate of the previous generation (kept at 14°C to avoid starvation), or up to a maximum of three generations prior. After 10 generations, lines were cryopreserved (*31*) at–80°C until the reproductive output assays. (**A**) Mean proportion of plates surviving per generation of selfing in control (solid line) and EMS (dashed line) lines. (**B**) simulation results for constant-effects model, $h = 0$; dashed line is the mean proportion of plates surviving per line (v); solid line is the proportion of mutations selectively lost (m_l), as functions of mutation effect s_m. Gray bar represents the 95% CI on v from the data, so values of s_m for which simulated v falls within it are compatible with the data; the range of proportion of mutations that may have been lost to selection can be inferred from the m_l values associated with these s_m values. Dotted gray line corresponds to the maximum parameter values consistent with data: $s < 10^{-3}$, $m_l < 0.06$. Simulations run under a variety of dominance coefficients ($0 \le h \le 0.5$) or assuming γ-distributed s_m yield almost identical limits on s and m_l.

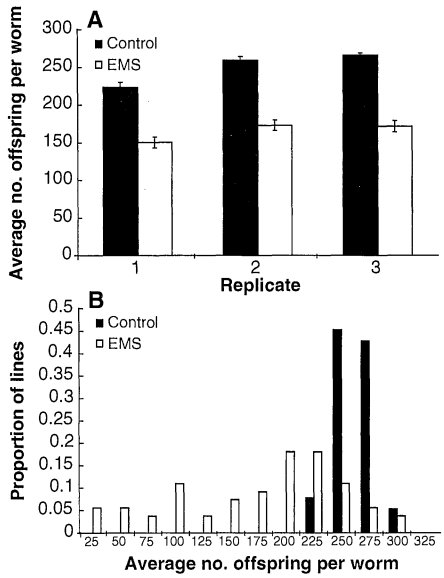

Fig. 2. (**A**) Mean productivity for the three assays. (**B**) Distribution of line means, averaged over replicates, for productivity. After mutagenesis, the cryopreserved lines were thawed, then individual replicates within each line were maintained for three generations. Productivity was measured contemporaneously in three replicates from each mutant and control line. In each replicate, four worms were allowed to lay eggs on a plate for ~3 hours, then removed. After 48 hours, a single randomly picked worm was transferred onto a new plate, then transferred 48 hours later and at 24-hour intervals for the entire reproductive period. The offspring were counted manually 48 to 72 hours after the parental transfer. Each counter assayed one replicate per line, and the entire assay was performed three times. Lines were randomized and counters were unaware of line identity. Analysis of variance was used to estimate the between-line variance for productivity; additional effects fitted were measurer, assay number, and their interaction, which was nonsignificant. The between-line variance component was highly significant for the EMS lines ($P < 0.001$) but not the controls ($P > 0.6$). The EMS-induced mutational heritability was $V_M/V_E = 1.0$ (±0.22), where $V_M = V_G/2$ and V_E is the environmental variance (2426 worms^2). The control and EMS mean productivities were 248.5 and 163.2 worms, respectively.

Table 2. Estimates of mutation rates and effects with U_I variable.

Method	Model	$\hat{U}_I$ (SE)	$\hat{s}$ (SE)	$\hat{\beta}$
Moments (*3*)	Equal effects	1.4 (0.36)	24% (3.9)	–
ML (*23*)	Equal effects	1.6 (0.21)	22% (1.9)	–
ML	γ distribution	<2.5	>15%	>1.6

Table 3. Estimates of mutation rates and effects, and fit of models to the data, with U_l fixed at 45 and ML analysis (*23*).

Model	$\hat{U}_{l1}$ (SE)	$\hat{s}_1$ (SE)	$\hat{U}_{l2}$	$\hat{s}_2$	$\hat{\beta}$ (SE)	Log *L*
Equal effects	45*	0.99% (0.04)	–	–	–	−160
γ distribution	45*	0.79% (0.05)	–	–	0.029 (0.005)	−3.8
Two classes of equal effects	1.6 (0.17)	22% (0.9)	43.4*	<0.074%	–	0

*Constrained by the assumption of fixed U_l.

first accounting for an average of 1.6 mutations per line (these had effects of 22%, as for the single-class equal-effects model under ML), whereas the remaining 43.4 mutations have virtually zero effect (Table 3). The maximum fitness effect that this class of weakly deleterious mutations can take is only 0.07% (Table 3). The distribution of mutation effects is therefore multimodal. If a number of deleterious mutations other than 45 is assumed, the estimated number and mean effect of strongly deleterious mutations remains the same ($\hat{U}_{l1} = 1.6$, $\hat{s}_1 = 22\%$), whereas the maximum effect of the weakly deleterious mutations changes proportionately (for example, $U = 20$, $\hat{s}_2 < 0.17\%$; $U = 80$, $\hat{s}_2 < 0.04\%$).

Distributions of EMS-induced and spontaneous (*24*) mutation effects on productivity therefore appear to be remarkably similar: The model of equal effects fits the data better than a γ distribution model in both cases, and $\hat{s}$ was 21% (±4%) for spontaneous mutations (*24*) compared to 22% (±2%) here. Our results imply that the spontaneous genomic deleterious mutation rate *U*, 0.0026 (±0.0012) per haploid (*24*), could have been underestimated by a factor of at least 28 (that is, 45/1.6), and that *U* is therefore closer to ~0.07. Our estimate for the mean mutation effect under an equal effects model is also nonsignificantly different from the positive mean mutational effect on productivity measured in a more recent spontaneous mutation accumulation experiment in *C. elegans* (*25*), that is, $s = -24\% \pm 23\%$.

Diploid *U* must be greater than 1 for sexual reproduction to be maintained by deleterious mutations (*1, 26*). Because *C. elegans* reproduces primarily as a self-fertilizing hermaphrodite, it does not pay the full twofold cost of sex. However, our corrected estimate for the spontaneous deleterious mutation rate specific to protein-coding genes (~0.14 mutations per diploid per generation) leads to the prediction that related sexual species would have higher mutation rates if deleterious mutations explain sex (although a maximum corrected *U*, assuming all 220 EMS-induced nucleotide changes in the genome are deleterious, is 0.72 per diploid). The high frequency of mutations of very small effect also has implications for the rate of fitness loss due to mutation accumulation. It has been assumed that mutations with fitness effects on the order of 1% are common (*2, 26, 27*), but our finding that >96% of mutations are undetectable in the laboratory, and have fitness effects of less than 0.07%, brings the validity of this assumption into question. We have inferred that there is a large class of deleterious mutations with tiny effects in the laboratory. Whether their effects are magnified in harsher natural environments remains to be determined; evidence for strong interactions between deleterious mutation effects and environmental conditions is equivocal (*5, 28*). It is clear, however, that mutation accumulation experiments may substantially underestimate mutation rates, and this will be undetected unless the number of events at the DNA level can be estimated.

References and Notes

1. A. S. Kondrashov, *Nature* **336**, 435 (1988).
2. R. Lande, *Evolution* **48**, 1460 (1994); M. Lynch, J. Conery, R. Burger, *Am. Nat.* **146**, 489 (1995).
3. J. F. Crow and M. J. Simmons, in *The Genetics and Biology of* Drosophila, M. Ashburner *et al.*, Eds. (Academic Press, London, 1983), vol. 3C, pp. 1–35.
4. P. D. Keightley, *Genetics* **144**, 1993 (1996); A. García-Dorado, *Evolution* **51**, 1130 (1997).
5. J. D. Fry, P. D. Keightley, S. L. Heinsohn, *Proc. Natl. Acad. Sci. U.S.A.* **96**, 574 (1999).
6. A. S. Kondrashov and J. F. Crow, *Hum. Mutat.* **2**, 229 (1993); A. Eyre-Walker and P. D. Keightley, *Nature* **397**, 344 (1999).
7. P. Anderson, in Caenorhabditis elegans*: Modern Biological Analysis of an Organism*, H. F. Epstein and D. C. Shakes, Eds. (Academic Press, London, 1995), pp. 31–54.
8. A. Bejsovec and P. Anderson, *Genes Dev.* **2**, 1307 (1988).
9. R. H. Waterston, *Genetics* **97**, 307 (1981).
10. J. Hodgkin, *ibid.* **111**, 287 (1985).
11. K. Kondo, B. Makovec, R. H. Waterston, *J. Mol. Biol.* **215**, 7 (1990).
12. The *C. elegans* Sequencing Consortium, *Science* **282**, 2012 (1998).
13. Y. Nakamura, T. Gojobori, T. Ikemura, *Nucleic Acids Res.* **27**, 292 (1999).
14. M. Stenico, A. T. Lloyd, P. M. Sharp, *ibid.* **22**, 2437 (1994).
15. S. A. Shabalina and A. S. Kondrashov, *Genet. Res.*, in press.
16. D. G. George, W. C. Barker, L. T. Hunt, *Methods Enzymol.* **183**, 333 (1990).
17. E. K. Davies, A. D. Peters, P. D. Keightley, data not shown.
18. To estimate the number of mutations selectively lost during inbreeding, we performed computer simulations mimicking the experimental design. Poisson means per haploid of one near-lethal mutation (*21*) (with effect $s_l = 0.9$), and 45 mutations of minor effect [with effects either constant (s_m) or drawn from a γ distribution], were initially assigned to a line. Genetic map positions were assigned by choosing random physical positions on random chromosomes, then converting physical position to map position using functions based on "Marey maps" [T. M. Barnes, Y. Kohara, A. Coulson, *Genetics* **141**, 159 (1995)]. The recombinant frequency per chromosome per generation was exactly 0.5; crossovers occurred at random locations. One selfed offspring was chosen per parent to reproduce, and its probability of survival was calculated as $v_c \times \Pi_i(1 - hs_i) \times \Pi_j(1 - s_j)$, where v_c is the mean observed viability for the control lines (0.98), *i* and *j* are indices of heterozygous and homozygous mutations, respectively, *s* is the mutation effect, and *h* is the dominance coefficient. Near-lethal mutations ($s > 0.5$) were assumed to be fully recessive ($h = 0$); *h* was constant for all other mutations in a given simulation. If an offspring failed to survive, one of two backup offspring was used; if neither backup survived, an offspring from the previous generation was used, to a maximum of three generations. One thousand replicates of the simulation were run for each of several values of s_m (or, under the γ distribution, scale parameter α and shape parameter β) and *h*. For each set of parameter values, *v*, the mean proportion of plates surviving per line, and m_l, the mean proportion of mutations lost to selection per line, were calculated. Those parameter values yielding *v* within the observed 95% CI were considered consistent with the observed results; the m_l values associated with these runs yield an estimated range of the average number of mutations lost to selection.
19. To measure the mutation rate at the *unc-22* locus, we screened 70 plates of adult progeny of mutagenized worms and 14 plates of controls, each containing an average of ~10,000 worms, for *unc-22* mutants by exposing them to 1% nicotine solution, conditions in which heterozygotes twitch rapidly but wild types are paralyzed. Putative mutants were allowed to self-fertilize on separate plates to confirm segregation of *unc-22*. Examination of the data revealed that the proportion of *unc-22* was significantly lower on plates with larger numbers of worms, suggesting that the number of mutants on crowded plates was underestimated. To control for this, we performed a stepwise quadratic regression with the frequency of *unc-22* mutants as the dependent variable and the number of worms per plate as the independent variable. The final model included significant terms for the intercept ($t = 7.2$, $p \leq 5.7 \times 10^{-10}$), linear ($t = -3.4$, $p \leq 0.0012$), and quadratic ($t = 2.2$, $p \leq 0.031$) terms [overall $F(2, 69) = 13.8$; $p \leq 9.3 \times 10^{-6}$; adjusted $R^2 = 0.27$]. The *y* intercept was then taken as the corrected estimate of *unc-22* mutation rate.
20. D. Eide and P. Anderson, *Genetics* **109**, 67 (1985).
21. R. W. Rosenbluth, C. Cuddeford, D. L. Baillie, *Mutat. Res.* **110**, 39 (1983).
22. In *Drosophila*, the rates of detectable mutation for viability and other life history traits under an equal-effects model are also similar to the lethal mutation rate under EMS mutagenesis (*29*).
23. In the ML inference of the distribution of mutation effects (*29*), the number of mutations per EMS line was assumed to be a random variable, *n*, sampled from a Poisson-distribution parameter U_l. The productivity of a replicate *i* was $M - \Sigma_{j=1}^{n} s_j + f_i + e_i$, where *M* is the population mean, f_i is the fixed effect of assay + counter, e_i is a normally distributed environmental effect of mean 0 and variance σ^2_e, and s_j is a mutation effect that takes the following values: *s* (equal-effects model); s_1 with probability *p* or s_2 with probability $1 - p$ (two equal effects); and a random deviate from a γ distribution with shape and scale parameters β and β/*s*, respectively. Control lines were included in the analysis with *n* assumed to be zero. Models were fitted in which U_l was a variable parameter (Table 2) or was fixed at 45 (Table 3). Standard errors of estimates (SEs) for the equal-effects model with U_l variable were obtained by bootstrapping the data, by line, 500 times. For models with U_l fixed, SEs were obtained from a quadratic approximation to profile likelihoods. Estimates marked ">" or "<" are the lowest or highest values compatible with

the data under likelihood ratio tests; these are asymptotically equivalent to 95% confidence limits. Log L is the difference in natural log likelihood from that of the model with two classes of equal deleterious effects, which has the same likelihood as the one-equal-effect model with U_1 variable. In the two-equal-effects model, a positive value for s_2 gave a higher likelihood than $s = 0$, but the difference in log likelihood was nonsignificant.

24. P. D. Keightley and A. Caballero, *Proc. Natl. Acad. Sci. U.S.A.* **94**, 3823 (1997).
25. L. Vassilieva and M. Lynch, *Genetics* **151**, 119 (1999).
26. A. S. Kondrashov, *J. Theor. Biol.* **175**, 583 (1995).
27. J. F. Crow, *Proc. Natl. Acad. Sci. U.S.A.* **94**, 8380 (1997).
28. A. S. Kondrashov and D. Houle, *Proc. R. Soc. London* **258**, 221 (1994); S. A. Shabalina, L. Y. Yampolsky, A. S. Kondrashov, *Proc. Natl. Acad. Sci. U.S.A.* **94**, 13034 (1997); P. D. Keightley, A. Caballero, A. García-Dorado, *Curr. Biol.* **8**, R235 (1998).
29. P. D. Keightley and O. Ohnishi, *Genetics* **148**, 753 (1998).
30. A. Bejsovec and P. Anderson, *Cell* **60**, 133 (1990).
31. J. Sulston and J. Hodgkin, in *The Nematode* Caenorhabditis elegans, W. B. Wood, Ed. (Cold Spring Harbor Laboratory Press, Cold Spring Harbor, NY, 1988), pp. 587–606.
32. We thank A. Eyre-Walker, D. Charlesworth, M. Blaxter, T. Bataillon, W. G. Hill, and C. S. Haley for helpful comments, and the UK Biotechnology and Biological Sciences Research Council and the Royal Society for support.

30 April 1999; accepted 4 August 1999

A Piston Model for Transmembrane Signaling of the Aspartate Receptor

Karen M. Ottemann,[1]*† Wenzhong Xiao,[2]* Yeon-Kyun Shin,[2]‡ Daniel E. Koshland Jr.[1]‡

To characterize the mechanism by which receptors propagate conformational changes across membranes, nitroxide spin labels were attached at strategic positions in the bacterial aspartate receptor. By collecting the electron paramagnetic resonance spectra of these labeled receptors in the presence and absence of the ligand aspartate, ligand binding was shown to generate an ~1 angstrom intrasubunit piston-type movement of one transmembrane helix downward relative to the other transmembrane helix. The receptor-associated phosphorylation cascade proteins CheA and CheW did not alter the ligand-induced movement. Because the piston movement is very small, the ability of receptors to produce large outcomes in response to stimuli is caused by the ability of the receptor-coupled enzymes to detect small changes in the conformation of the receptor.

Cells receive signals from the outside world by way of receptors that span the membrane. Although some receptors transmit information across the membrane by means of an ion channel that allows ions into the cell, most receptors do not transmit material across the membrane. Rather, these receptors undergo conformational changes induced by the ligand or stimulus that interacts with the exterior part of the receptor, and these conformational changes travel across the membrane to the cytoplasmic portion of the receptor. The types of conformational changes used by receptors to carry out transmembrane signaling are not known.

To distinguish among alternative models proposed for transmembrane signaling, we developed a strategy in which the distances between appropriately placed spin labels would give different results for different models (*1*) (Fig. 1). In this procedure, spin-labeling electron paramagnetic resonance (EPR) spectroscopy (*2*) was combined with the use of a spectroscopic ruler (*3, 4*). Spin labeling has been used to describe qualitative protein structures (*5, 6*) and has subsequently been developed for quantitative assessment of protein movements and applied to several proteins (*4, 7, 8*), including the aspartate receptor (*9*). In a hypothetical example (Fig. 1), a model of transmembrane signaling that depended on an association-dissociation, as well as one that required a scissors movement, would move residue a closer to b and c. A ligand-induced piston motion would move residue a closer to b, but further from c. A rotation mechanism would move a further from b, but closer to c. A see-saw motion would move b and c both further from a. Thus, judicious placement of spin labels allows an analysis that can distinguish among models.

This strategy was applied to the bacterial aspartate receptor, a receptor with a structure similar to that of many other receptors that contain one-two transmembrane domains per subunit and function as oligomers [such as the insulin receptor, the epidermal growth factor receptor (EGFR), and the cytokine receptors] (*10–12*). The aspartate receptor and its homologs are used by bacteria to navigate through spatial gradients of nutrients and toxic substances, using detection of temporal gradients to modulate swimming behavior (*13–17*). Although the aspartate receptor has been studied in detail, the mechanism of signal transduction has remained elusive. Disulfide cross-linking experiments have suggested that aspartate triggers global changes in the receptor (*18*). Several mechanistic models, postulated on the basis of fragments of either the ligand-binding domain (*19–22*) or the cytoplasmic domain (*23, 24*), have been proposed. Ligand binding does not affect the dimerization state of the aspartate receptor (*25*), and receptors that are disulfide cross-

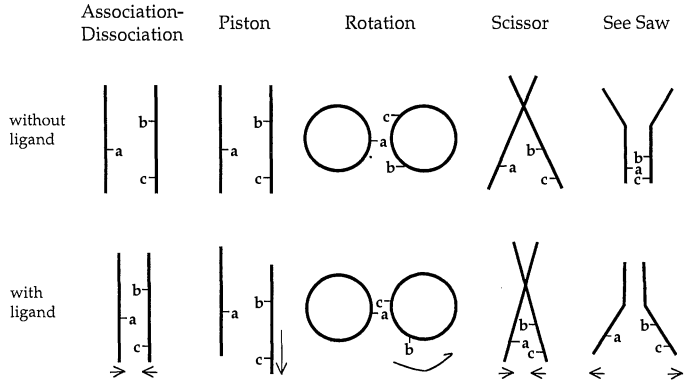

Fig. 1. Postulated models for transmembrane signaling. General schemes for possible ligand-generated movements in transmembrane receptors (*1*). The thick lines represent receptor transmembrane helices. The view is from the side, except in the rotation diagram where the view is from the end of the helices. Any of these motions could occur between two helices in separate subunits, or between two helices within one subunit. The letters represent amino acid side chains where labels could be attached. The rotation model could have results similar to those seen in the piston model, but the labels could be placed such that they would distinguish between models, as shown.

[1]Department of Molecular and Cell Biology and [2]Department of Chemistry, University of California, Berkeley, CA 94720, USA.

*These authors contributed equally to this work.
†Present address: Departments of Biology and Environmental Toxicology, University of California at Santa Cruz, CA 95064, USA.
‡To whom correspondence should be addressed. E-mail: shin@cchem.berkeley.edu (Y.-K.S.); dek@uclink4.berkeley.edu (D.E.K).